
Joint Training of Low-Precision Neural Network with Quantization Interval Parameters

Sangil Jung
sang-il.jung
@samsung.com

Changyong Son
cyson
@samsung.com

Seohyung Lee
seoh.lee
@samsung.com

Jinwoo Son
jwoo.son
@samsung.com

Youngjun Kwak
yjk.kwak
@samsung.com

Jae-Joon Han
jae-joon.han
@samsung.com

Changkyu Choi
changkyu_choi
@samsung.com

Abstract

Optimization for low-precision neural network is an important technique for deep convolutional neural network models to be deployed to mobile devices. In order to realize convolutional layers with the simple bit-wise operations, both activation and weight parameters need to be quantized with a low bit-precision. In this paper, we propose a novel optimization method for low-precision neural network which trains both activation quantization parameters and the quantized model weights. We parameterize the quantization intervals of the weights and the activations and train the parameters with the full-precision weights by directly minimizing the training loss rather than minimizing the quantization error. Thanks to the joint optimization of quantization parameters and model weights, we obtain the highly accurate low-precision network given a target bitwidth. We demonstrated the effectiveness of our method on two benchmarks: CIFAR-10 and ImageNet.

1 Introduction

Deep Convolutional Neural Networks (DCNNs) have achieved a great improvement in various computer-vision applications such as image classification [1; 2; 3], object detection [4; 5; 6] and semantic segmentation [7]. As DCNNs deepen and broaden, the expressive power increases and the performance improves. However, this also increases the required memory usage to store the model as well as computational complexity.

To embed DCNNs into resource-limited devices such as mobile phones, reducing both the model size and the computational complexity is inevitable. One way to achieve this goal is reducing bit-precision for weights or activations. Convolutional operations can be computed efficiently by utilizing bit-wise operations which is composed of logical operations (and, xnor) and bitcount operations if the bitwidth of weights and activations become low enough. Converting the floating-point real values into the fixed-point integer values requires Q-format conversion which inherently includes a quantization process, which results in the errors between the original values and the associated quantized values determined by the target bitwidth. Generally, reducing the bitwidth of the weights and the activations degrades the performance, e.g., classification accuracy for image classification.

To maintain full-precision performance while reducing bitwidth, most of the previous work has attempted to find the optimal quantized values which minimize the quantization errors so that the converted low-precision model generates the similar output values to the ones from the full-precision model. The quantization range (e.g., maximum) is deterministically set from the data, thus the quantization error depends on the bit-precision. That is, reducing the bitwidth results in the

degradation of the quantized model due to the low quantization resolution. On the other hand, the quantization range might be set by truncating small values and cutting-off large values which can be viewed as pruning and clipping, respectively. Depending on the bit-precision, the quantization range(interval) that can significantly affect performance may vary.

Weight pruning scheme not only reduces the model size but also acts as a regularizer for enhancing model robustness [8]. Note that the pruning removes the weight parameters, the value which is close to zero. Quantization also makes the weight values, smaller than the lower bound, be zero. Similarly, the activation pruning acts as removing some small activation values which is insignificant to the performance. In case of activation function, the output of ReLU is in the range of $[0, \infty)$. Therefore, the upper bound of the quantizing intervals set by the possible largest values enlarges the quantization interval which results in large quantization errors and thus may degrades the classification performance. A few works has proposed to bound activation values by introducing variants of activation functions [9; 10]. We notice that setting the upper bound of activation during quantization may improve the performance by reducing quantization error. Similarly, this upper bound of quantization can also be applied to the weight quantization.

Based on the above observations on pruning and clipping, the appropriate quantization interval is important to preserve the accuracy of low-precision network. We parameterize this quantization interval with trainable parameters so that pruning and clipping can be performed simultaneously during training. We apply these trainable quantization interval parameters both to weights and to activations and jointly learn them with full-precision model weights. Note that the full-precision weights and quantization parameters are preserved and updated only in the training stage, and then the quantized weights are utilized in the inference stage. For learning the interval parameters, we focus on minimizing training loss rather than minimizing quantization errors. In addition, we utilize the knowledge distillation technique [11; 12; 13; 14] to find the model which achieve the best classification accuracy. The knowledge distillation is a method of compressing ensemble models into a single model or a complex model into a simpler model. Recently, the distillation techniques have been applied to improve performance on training low-precision networks [13; 14].

In summary, our main contributions are:

- We introduce the trainable quantization interval parameters that simultaneously perform pruning and clipping during network training.
- We apply the quantization interval parameters to both weights and activations, and jointly train them with the full-precision model weights.
- Our method achieved the state-of-the-art classification accuracies both on CIFAR-10 and ImageNet with extremely low-bitwidth (2, 3, and 4-bit) networks.

The rest of this paper is organized as follows. Some work related to ours is reviewed in Section 2. The proposed parameterization and the optimization method are described in detail in Section 3. Experimental results that show the superiority of our method are given in Section 4.

2 Related Work

We review the related work in the aspect of low-precision networks. Low-precision networks have two benefits: model compression and operation acceleration. Some work lightened the network model by reducing bitwidth of model weights: BinaryConnect (BC) [15], Binary-Weight-Network (BWN) [16], Ternary-Weight-Network (TWN) [17] and Trained-Ternary-Quantization (TTQ) [18]. BC uses either deterministic or stochastic methods for binarizing the weights which are $\{-1, +1\}$. BWN approximates the full-precision weights as the scaled bipolar($\{-1, +1\}$) weights, and find the scale in a closed form solution. TWN utilized the ternary($\{-1, 0, +1\}$) weights with scaling factor which is trained in training phase. TTQ uses the same quantization method but the different scaling factors are learned on the positive and negative sides. These methods are solely about weight quantization, especially for binary or ternary, and do not consider the activation quantization.

In order to utilize the bit-wise operation for convolution, both weights and activations should be quantized. Binarized-Neural-Network(BNN) [19] binarized the weights and activations to $\{-1, +1\}$ in the same way as BC, and used these binarized values for computing gradients. In addition to the BWN, XNOR-Net [16] also conducts activation binarization with a scaling factor where the

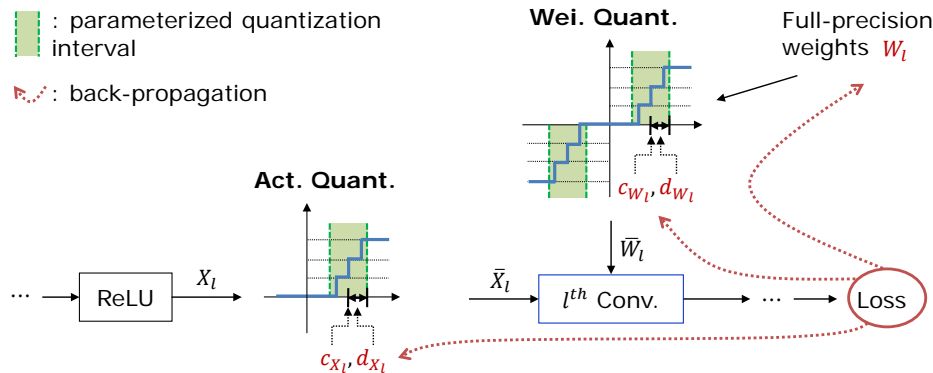


Figure 1: The l^{th} convolution layer of our low-precision network. The quantized weights \bar{W}_l and activations \bar{X}_l are acquired using the parameterized intervals and the given bitwidth. The interval parameters $(c_{W_l}, d_{W_l}, c_{X_l}, d_{X_l})$ are trained together with the full-precision weights W_l via backpropagation.

scaling factor is obtained in closed form solution. DoReFa-Net [9] performs a bit-wise operation for convolution by quantizing both weight and activation with multiple-bits rather than the bipolar type. They adopted various activation functions to bound the activation values. The weights were transformed by the hyperbolic tangent function and then normalized by the maximum values before quantization. Half-Wave-Gaussian-Quantization (HWGQ) [20] exploited the statistics of activations and proposed activation function variants of ReLU which constrains the unbounded values. Both DoReFa-Net and HWGQ use upper bounds for the activation but they are fixed during training and do not consider the trainable quantization interval. PACT [10] proposed a parameterized clipping activation function where the clipping parameter is obtained during training. However, it does not consider the pruning that suppresses near-zero values, and the weight quantization is deterministic as in DoReFa-Net. We propose the trainable quantization interval parameters which perform pruning and clipping simultaneously during training, and by applying this parameterization both for weights and activation quantization we keep the classification accuracy on par with the one of the full-precision network while reducing the bitwidth significantly.

3 Method

This section describes the parameterization of the quantization interval and the training method for the interval parameters together with the full-precision weights. Fig. 1 shows an exemplar l^{th} convolutional layer with the quantization operations of our low-precision network. Given a certain bitwidth, both the full-precision weights W_l and the full-precision activations X_l are quantized by the following quantizers where the intervals are parameterized by the center c_* ($* \in W_l, X_l$) and the distance d_* from the center. Then the quantized weights \bar{W}_l and the quantized activation \bar{X}_l are convolved by utilizing the bit-wise operations. Loss is computed through the forward pass, and then the interval parameters are updated together with full precision weights via backpropagation. This implies that the interval parameters are obtained by minimizing training loss rather than minimizing quantization error. Note that the full-precision weight W_l and the quantization parameters (c_{W_l}, d_{W_l}) are preserved and updated only in the training stage. For inference, the model only stores the quantized weights and the interval parameters for activation quantization.

3.1 Quantization via parameterized interval

Quantization is an approximation of full-precision values into a set of discrete values which can be represented by fixed-point integers and scale factors. Formally, the quantized value \bar{v} is derived by the (positive) real-value v as follows:

$$\bar{v} = \frac{\lfloor (v/sc) \cdot q_L \rfloor}{q_L} \cdot sc, \quad (1)$$

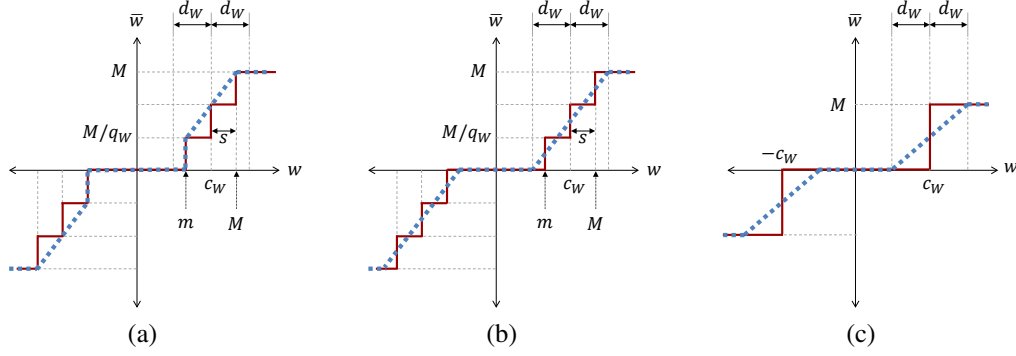


Figure 2: The mapping functions for weight quantization. The dotted blue lines represent the intermediate forward function for quantization in (a); the approximated function for backward pass for $N_W \geq 3$ in (b) and for $N_W = 2$ in (c), respectively. The s represents the step size ($= 2d_W/q_W$).

where the sc denotes the scale factor that normalizes v to the range $[0, 1]$ and q_L is the number of the quantization levels. The $\lfloor \cdot \rfloor$ indicates the *floor* operation that throws away below the decimal point.

Weight quantization The interval parameters (c_{W_l}, d_{W_l}) are defined for each layer. Let N_{W_l} be the number of bits to represent the quantized weights \bar{W}_l of the l^{th} layer. For simplicity of notation, the subscript l is ignored which indicates l^{th} convolutional layer in the following. Given N_W , the number of the quantization levels q_W is computed as $2^{N_W} - 1$. For example, if $N_W = 3$, then $q_W = 3$ which means that the set of quantization values are $\{-M, -\frac{2}{3}M, -\frac{1}{3}M, 0, \frac{1}{3}M, \frac{2}{3}M, M\}$ where M is the scaling factor (Fig. 2(a, b)). Given c_W and d_W , the positive side interval $(c_W - d_W, c_W + d_W)$ is uniformly quantized at the q_W level and the negative side interval $(-c_W - d_W, -c_W + d_W)$ is also quantized in the same way as the positive side.

To conduct quantization in the forward pass, we first introduce a mapping function from w to \hat{w}_F in order to incorporate pruning and clipping of the weights (the dotted blue line in Fig. 2(a)).

Denote w as each element of W . The mapping function is defined as follows:

$$\hat{w}_F = \begin{cases} 0 & |w| < m \\ M \cdot \text{sign}(w) & |w| > M \\ \alpha w + \beta' \cdot \text{sign}(w) & m \leq |w| \leq M, \end{cases} \quad (2)$$

where

$$\begin{aligned} m &= c_W - d_W + d_W/q_W \\ M &= c_W + d_W - d_W/q_W \\ \alpha &= 0.5M/d_W \\ \beta' &= M - 0.5M^2/d_W. \end{aligned} \quad (3)$$

Note that the mapping function prunes the values less than m to be zero and cuts off the magnitudes of the values larger than M to be M . Then the quantized weights \bar{w} from Eq. 1 can be written as:

$$\bar{w} = \frac{\lfloor (|\hat{w}_F|/M) \cdot q_W \rfloor}{q_W} \cdot M \cdot \text{sign}(w), \quad (4)$$

that is derived from Eq. 1.

In this way, the parameterized interval prunes and bounds the weights by suppressing the near-zero weights ($|w| < m$) to zero and clipping the absolute values of weights to M .

During backward pass, the loss cannot be back-propagated due to the discontinuities in the quantization function. Thus, we approximate the quantization function as a piecewise linear function (the dotted blue line in Fig. 2(b)). Formally, the function is defined as:

$$\hat{w} = \begin{cases} 0 & |w| < c_W - d_W \\ M \cdot \text{sign}(w) & |w| \geq c_W + d_W \\ \alpha w + \beta \cdot \text{sign}(w) & c_W - d_W \leq |w| \leq c_W + d_W, \end{cases} \quad (5)$$

where α is the same as in Eq. 3 and $\beta = \beta' - 0.5M/q_W$.

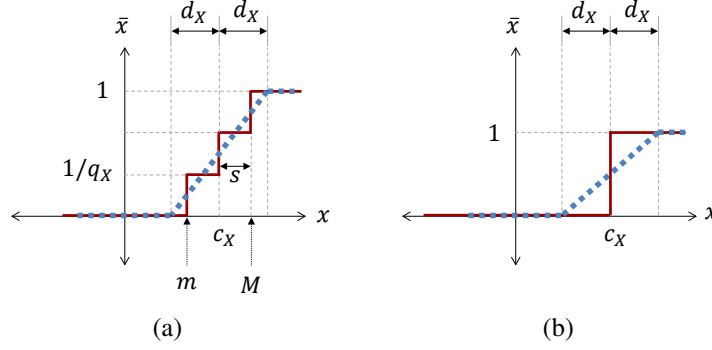


Figure 3: Activation quantization. The dotted blue lines represent the approximated function for quantization for (a) $N_X \geq 2$ and (b) $N_X = 1$, respectively.

Then the gradients of \hat{w} with respect to w , a and b can be computed as follows:

$$\begin{aligned} \frac{\partial \hat{w}}{\partial w} &= \begin{cases} 0 & |w| < c_W - d_W \text{ or } |w| > c_W + d_W \\ \alpha & c_W - d_W \leq |w| \leq c_W + d_W, \end{cases} \\ \frac{\partial \hat{w}}{\partial c_W} &= \begin{cases} 0 & |w| < c_W - d_W \\ \frac{\partial M}{\partial c_W} \cdot \text{sign}(w) & |w| > c_W + d_W \\ \frac{\partial \alpha}{\partial c_W} w + \frac{\partial \beta}{\partial c_W} \cdot \text{sign}(w) & c_W - d_W \leq |w| \leq c_W + d_W, \end{cases} \quad (6) \\ \frac{\partial \hat{w}}{\partial d_W} &= \begin{cases} 0 & |w| < c_W - d_W \\ \frac{\partial M}{\partial d_W} \cdot \text{sign}(w) & |w| > c_W + d_W \\ \frac{\partial \alpha}{\partial d_W} w + \frac{\partial \beta}{\partial d_W} \cdot \text{sign}(w) & c_W - d_W \leq |w| \leq c_W + d_W, \end{cases} \end{aligned}$$

where

$$\begin{aligned} \frac{\partial M}{\partial c_W} &= 1, & \frac{\partial \alpha}{\partial c_W} &= 0.5d_W, & \frac{\partial \beta}{\partial c_W} &= -c_W/d_W + 0.5/q_W, \\ \frac{\partial M}{\partial d_W} &= 1 - 1/q_W, & \frac{\partial \alpha}{\partial d_W} &= -0.5c_W/d_W^2, & \frac{\partial \beta}{\partial d_W} &= 0.5c_W^2/d_W^2 - 0.5/q_W + 0.5. \end{aligned} \quad (7)$$

The M , α and β are differentiable functions with respect to w , c_W and d_W , and their derivations are straight-forward.

In case of $N_W = 2$ ($q_W = 1$), the forward quantization is defined only by c_W :

$$\bar{w} = \begin{cases} 0 & |w| < c_W \\ M \cdot \text{sign}(w) & |w| \geq c_W. \end{cases} \quad (8)$$

Thus, the d_W is meaningless for the forward pass but it is still valid and is trainable in backward pass because the approximated quantization function (Fig. 2(c)) is defined by c_W and d_W . The gradients are the same as in Eqs. 6 and 7 with $q_W = 1$.

Activation quantization Activation quantization can be similarly formulated to the weight quantization but differs from the weight quantization in two aspects. First, the only positive side is considered because the range of the full-precision activations x is ≥ 0 due to characteristics of ReLU function. Thus, the number of the quantization levels q_X is computed as $2^{N_X} - 1$ where N_X denotes the number of bits for quantization; if $N_X = 2$, then $q_X = 3$ which means that the set of the quantized values are $\{0, \frac{1}{3}, \frac{2}{3}, 1\}$. Second, the activation value is normalized by the upper bound so that the activation value can be quantized in the range of $[0,1]$ which improves training stability. Fig. 3 shows the activation quantization and the approximated function \hat{x} for backward pass (the blue dotted lines):

$$\hat{x} = \begin{cases} 0 & x < c_X - d_X \\ 1 & x > c_X + d_X \\ \alpha x + \beta & c_X - d_X \leq x \leq c_X + d_X \end{cases} \quad (9)$$

where

$$\begin{aligned}
 m &= c_X - d_X + d_X/q_X \\
 M &= c_X + d_X - d_X/q_X \\
 \alpha &= 0.5/d_X \\
 \beta &= -0.5c_X/d_X + 0.5
 \end{aligned}
 \tag{10}$$

Then the gradients of \hat{x} with respect to x , c_X and d_X are easily computed as:

$$\frac{\partial \hat{x}}{\partial x} = \begin{cases} 0 & x < c_X - d_X \text{ or } x \geq c_X + d_X \\ 0.5/d_X & c_X - d_X \leq x \leq c_X + d_X \end{cases}
 \tag{11}$$

$$\frac{\partial \hat{x}}{\partial c_X} = \begin{cases} 0 & x < c_X - d_X \text{ or } x \geq c_X + d_X \\ -0.5/d_X & c_X - d_X \leq x \leq c_X + d_X \end{cases}
 \tag{12}$$

$$\frac{\partial \hat{x}}{\partial d_X} = \begin{cases} 0 & x < c_X - d_X \text{ or } x \geq c_X + d_X \\ 0.5c_X/d_X^2 & c_X - d_X \leq x \leq c_X + d_X \end{cases}
 \tag{13}$$

3.2 Distillation

Distillation techniques [11] enable to compress the knowledge in an ensemble of models into a single model. A more complex model also can be compressed to a simpler model using knowledge distillation. In this sense, recently, the knowledge distillation was adopted to transfer the information of the full-precision networks to the lower-precision network [13]. The key idea of knowledge distillation technique is to utilize the logit of a teacher model for training a student model. Given an input image, the logit z indicates the un-normalized log probability value which can be extracting right before the softmax layer of the teacher model. Instead of temperature-based target generation [11; 13], we used the logit as target itself and minimize the mean-square error between the logits of the teacher and the student network as was done in [12]. The loss is defined as follows:

$$Loss = (1 - \lambda) \cdot CE(y, p) + \lambda \cdot MSE(z^T, z^P)
 \tag{14}$$

where $CE(y, p)$ is the cross-entropy loss and $MSE(z^T, z^P)$ is the mean-square error loss. The y , p , z^T and z^P indicate the ground-truth label, the predicted probability, the target logit and the predicted logit, respectively. The λ is the balancing hyper-parameter between CE and MSE , we used $\{0, 0.5, 1\}$ in our experiment. Utilizing knowledge distillation speeds up the convergence rate and improves the final classification accuracy.

4 Experiment results

To demonstrate the effectiveness of our method, we evaluated our method on two classification benchmark datasets: CIFAR-10 [21] and ImageNet [22].

4.1 CIFAR-10

The CIFAR-10 dataset [21] consists of 10 classes with 50,000 training images and 10,000 testing images where the image size is 32×32 . For evaluation, we used VGG-7 network¹ as was defined for TWN [17]. During training, the data augmentation was conducted as was done in [23; 3; 17]; 4 pixels were padded on each side, and a 32×32 crop was randomly sampled from the padded image or its horizontal flip. For testing, we only evaluated the single view of the original 32×32 image. Following the previous work [24; 9], we did not quantize the first and the last layers; quantizing these layers has been reported to deteriorate the accuracy significantly. We used stochastic gradient descent (SGD) optimization with momentum of 0.9, weight decay of 0.0002 and batch size of 128. For the convolutional layers, the initial learning rate was set to 0.1, then it decayed by multiplying 0.1 for every 60 epochs until maximum 200 epochs. For c_W , d_W and the fully-connected layers, we set the learning rate to be hundred times smaller than that of convolutional layers. In addition to the reduced learning rate of the fully-connected layers, we found that simple normalization of the quantized weight values in Eq. 2 increases the training stability, which improves the accuracy as well.

¹ $2 \times (128-C3) + MP2 + 2 \times (256-C3) + MP2 + 2 \times (512-C3) + MP2 + 1024-FC + \text{Softmax}$

Table 1: The testing accuracy (%) of our method on the CIFAR-10 dataset with VGG-7 network. (·) denotes the accuracy loss with respect to the full precision accuracy.

	A1W2	A1W3	A2W2	A3W3	A4W4	A5W5	A8W8	Full-Prec.
$\lambda = 0$	91.24 (+2.82)	90.85 (+3.21)	93.05 (+1.01)	92.96 (+1.10)	92.79 (+1.27)	93.47 (+0.59)	93.06 (+1.0)	94.06
$\lambda = 0.5$	92.89 (+1.17)	92.69 (+1.37)	93.90 (+0.16)	93.90 (+0.16)	93.89 (+0.17)	94.13 (-0.07)	94.18 (-0.12)	
$\lambda = 1$	92.92 (+1.14)	92.59 (+1.47)	93.83 (+0.23)	94.10 (-0.04)	93.85 (+0.21)	94.06 (0.0)	94.19 (-0.13)	

Table 2: The testing accuracy (%) of our methods and the previous method on the CIFAR-10 dataset with VGG-7 network. N_W and N_X denote the bitwidth for the quantization of weights and activations, respectively. Note that ternary, bipolar, and binary indicate $\{-1, 0, 1\}$, $\{-1, 1\}$, and $\{0, 1\}$, respectively. The accuracies of other methods are cited from the original papers, thus the implementation details could be different from ours.

	Method	N_W	N_X	Accuracy
	Full-Prec. (ours)	32	32	94.06
$N_W \leq 2$ & $N_X = 32$	Ours ($\lambda = 0.5$)	2 (ternary)		94.12 (-0.06)
	TTQ [18]	2 (ternary)		93.56
	TWN [17]	2 (ternary)	32	92.56
	BC [15]	1 (bipolar)		91.73
	BWN [16]	1 (bipolar)		90.12
$N_W \leq 2$ & $N_X = 8$	Ours ($\lambda = 0.5$)	2 (ternary)	8	93.96 (+0.10)
	WAGE [25]	2		93.22
$N_W \leq 2$ & $N_X \leq 4$	Ours ($\lambda = 0.5$)	2 (ternary)	4	94.11 (-0.05)
	Ours ($\lambda = 0.5$)	2 (ternary)	2	93.90 (+0.16)
	Ours ($\lambda = 0.5$)	2 (ternary)	1 (binary)	92.89 (+1.17)
	XNOR-Net [16]	1 (bipolar)	1 (bipolar)	89.83

Table 1 shows the test accuracy on the CIFAR-10 dataset with various bitwidths and λ where the λ is the degree of the distillation loss being used (Eq. 14). We used the bitwidths from 1 to 8 bits for the input activations and the ones from 2 to 8 bits for the weights. Note that our 2-bit weight is actually ternary ($\{-1, 0, 1\}$). In our notation, A1W2 represents that 1 and 2 bits are used for the activations and the weights, respectively. The ‘Full-Prec.’ indicates the full-precision accuracy which is 94.06%. Utilizing distillation loss ($\lambda = 0.5$ and 1) improves the accuracy, i.e., in case of 2A3W, the accuracies with $\lambda = 0.5$ and $\lambda = 1$ are 93.90% and 93.83%, respectively, while the accuracy with $\lambda = 0$ is 93.05%. On CIFAR-10 dataset, our method with the distillation loss preserves the full-precision accuracy even though the number of bits are reduced to 2 bits for both activations and weights; the accuracy is 93.90% so the accuracy decreases only by 0.16% ($\lambda = 0.5$). Even when we further reduce the bitwidth to binary for activation and ternary for weight (A1W2), the accuracy decreases only by 1.17% ($\lambda = 0.5$).

We also compared our results with the other methods (Table 2). To have a fair comparison with other methods which focus only on weight quantization (i.e., 2-bit weights and 32-bit activations), we conducted more experiments with 2-bit weights and various bitwidths (1, 2, 4, 8, and 32) of activation with $\lambda = 0.5$. The results of other methods are cited from the original papers, the implementation details might be different even though the network architecture is the same. Our method is superior to the other methods in terms of minimizing bitwidth while maintaining performance. Our method achieved the state-of-the-art low-bitwidth quantization, i.e., 2bit activation quantization and 2bit weight parameters while maintaining its performance.

To validate if the parameters of the intervals are trained properly, we plot the lower and the upper bounds across the entire epochs for the activations and the weights with 4-bit bitwidth in Fig. 4. Note that the bounds are converged to a certain values without any significant fluctuations. Figure

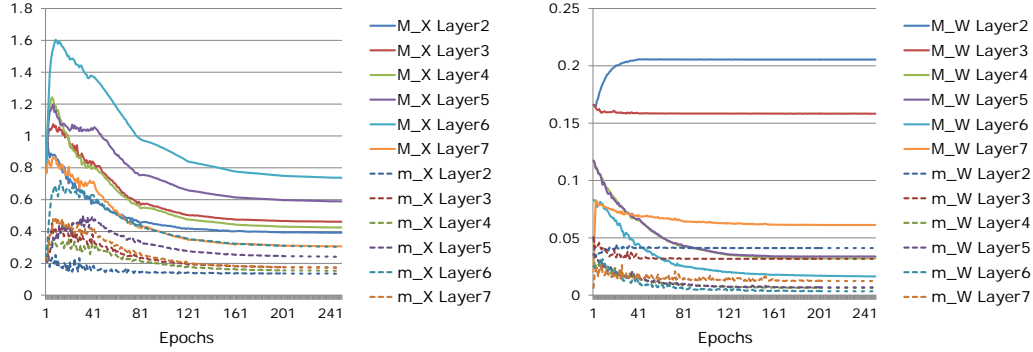


Figure 4: The lower-bound m and the upper-bound M for (a) activations and (b) weights.

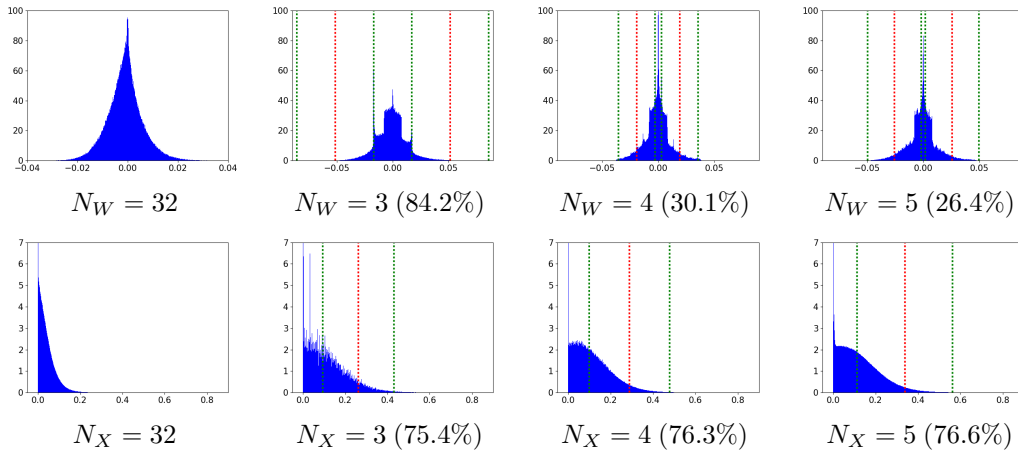


Figure 5: The exemplar distribution of the weights (top row) and activations (bottom row) of the trained full-precision model (left column) and the low-precision models (right three columns). The dotted red lines are the bounds of the interval and the dotted green lines are the center of the interval. (·) indicates the pruning ratio over the entire weights.

5 shows weight distributions and quantization intervals with different bitwidth. Interestingly, the shapes of the weight distributions trained with low bit-precision are quite different from the one with the full-precision model. In other word, the weight parameters are optimized differently dependent upon the given bitwidth. Another interesting point that we observe is that the pruning ratio increases from 26.4% to 84.2% as the bitwidth decreases from 5 bits to 3 bits. In case of activation, the distribution, the lower bound and the pruning ratio for each given bitwidth are similar to each other. Note that the pruning ratio is about 75%. As the pruning ratios for activations and weights increase, the computational complexity can decrease accordingly.

4.2 ImageNet

We also experimented with the large-scale ImageNet classification dataset [22] that consists of 1000 classes. The training/testing images were resized by making the shorter side to be 256 pixels. For training, the image was cropped randomly with the size of 224×224 and horizontally flipped with probability of 0.5. For testing, a single center-crop of 224×224 was used. We evaluated our method on two network architectures: ResNet-18 [26] and AlexNet [1]. For AlexNet, we modified the network by using batch-normalization layer after each convolution layer and removing the dropout layers and the LRN layers. For both the networks, we used SGD with the momentum of 0.9, the weight decay of 0.0001 and the batch size of 512 (4 GPUs). We used fine-tuning approach by adopting the higher-bitwidth weights for initialization which provides fast and stable convergence. The initial learning rate was set to 0.01 and decayed by a factor of 10 at epoch 20, 40, 60, and 80

Table 3: Top-1 accuracy (%) of our method with ResNet-18 and AlexNet models on the ImageNet dataset. The λ denotes the hyper-parameter in Eq. 14. (·) indicates the accuracy loss.

	ResNet-18			AlexNet		
	$\lambda = 0$	$\lambda = 0.5$	$\lambda = 1$	$\lambda = 0$	$\lambda = 0.5$	$\lambda = 1$
A2W2	65.4 (+3.8)	63.4 (+5.8)	60.3 (+8.9)	55.7 (+2.4)	54.5 (+3.6)	50.4 (+7.7)
A3W3	68.2 (+1.0)	68.1 (+1.1)	66.2 (+3.0)	58.5 (-0.4)	58.2 (-0.1)	56.3 (+1.8)
A4W4	69.3 (-0.1)	68.8 (+0.4)	68.1 (+1.1)	58.6 (-0.5)	58.5 (-0.4)	57.4 (+0.7)
Full-Prec.	69.2			58.1		

Table 4: Comparison with other existing methods: Top-1 accuracy (%) of ResNet-18 and AlexNet models on the ImageNet dataset. (·) indicates the accuracy loss. Note that the 2-bit weights of HWGQ [20], ours, and other methods are bipolar ($\{-1, 1\}$), ternary ($\{-1, 0, 1\}$), and 4-levels ($\{-1, -1/3, 1/3, 1\}$), respectively. Performance of DoReFa is cited from PACT [10].

		Ours ($\lambda = 0$)	PACT [10]	DoReFa [9]	HWGQ [20]	BalancedQ [27]
ResNet-18	A2W2	65.4 (+3.8)	64.4 (+5.8)	62.6 (+7.6)	59.6 (+7.7)	59.4 (+8.8)
	A3W3	68.2 (+1.0)	68.1 (+2.1)	67.5 (+2.7)	-	-
	A4W4	69.3 (-0.1)	69.2 (+1.0)	68.1 (+2.1)	-	-
	Full-Prec.	69.2	70.2	70.2	67.3	68.2
AlexNet	A2W2	55.7 (+2.4)	55.0 (+0.1)	53.6 (+1.5)	52.7 (+5.8)	55.7 (+1.4)
	A3W3	58.5 (-0.4)	55.6 (-0.5)	55.0 (+0.1)	-	-
	A4W4	58.6 (-0.5)	55.7 (-0.6)	54.9 (+0.2)	-	-
	Full-Prec.	58.1	55.1	55.1	58.5	57.1

with maximum 90 epochs for ResNet-18 and at epoch 5, 20, 30, 40 and 50 with maximum 60 epochs for AlexNet.

Table 3 shows the top-1 accuracy of our method on ImageNet dataset. While the training with the distillation technique is helpful for improving the accuracy on CIFAR-10 dataset, the distillation technique ($\lambda = 0.5$ or 1) has little or negative impact on the classification accuracies with ImageNet. Our low-bitwidth network without distillation ($\lambda = 0$) achieved the full-precision accuracy ($\leq 1\%$ accuracy losses) of ResNet-18 and AlexNet when the bitwidth is 4-bit or 3-bit for both weight and activation. Even with 2-bit weight and activation, the accuracy decreases by 3.8% and 2.4% for ResNet-18 and AlexNet, respectively.

We also compared our method with other existing methods such as PACT [10], DoReFa [9], HWGQ [20], and BalancedQ [27] (Table 4). Our method achieved the highest accuracy on both the network architectures for various bitwidths (2, 3, and 4 bits). We also achieved the smallest accuracy loss compared to the other methods for ResNet-18. For AlexNet, the accuracy losses of PACT and DoReFa are less than ours, but note that their base full-precision accuracy is quite lower ($\sim 3\%$) than ours.

5 Conclusion

We proposed a novel parameterization for low-precision network which consists of the quantization interval parameters and the weight parameters. The proposed method performs pruning and clipping during network training and optimizes jointly both the parameters by minimizing the classification loss rather than approximating the full-precision activations or weights. By determining the appropriate intervals for quantization, our method minimizes the degradation of classification accuracy given the reduced bitwidth of weights and activations. As a result, on CIFAR-10, given the number of bits, the optimized parameters were obtained while preserving the classification accuracies even when the number of bits is reduced to 2 bits with VGG-7 network. Even when the bitwidth is further reduced to the binary activations and the ternary weights, our model maintains the accuracy with a

reasonably small degradation. On ImageNet, our low-bitwidth networks with 2, 3, and 4 bits achieved the state-of-the-art classification accuracies for both ResNet-18 and AlexNet architectures.

References

- [1] Alex Krizhevsky, Ilya Sutskever, and Geoffrey E Hinton. Imagenet classification with deep convolutional neural networks. In *Advances in neural information processing systems*, pages 1097–1105, 2012.
- [2] Karen Simonyan and Andrew Zisserman. Very deep convolutional networks for large-scale image recognition. *arXiv preprint arXiv:1409.1556*, 2014.
- [3] Kaiming He, Xiangyu Zhang, Shaoqing Ren, and Jian Sun. Deep residual learning for image recognition. In *Proceedings of the IEEE conference on computer vision and pattern recognition*, pages 770–778, 2016.
- [4] Ross Girshick, Jeff Donahue, Trevor Darrell, and Jitendra Malik. Rich feature hierarchies for accurate object detection and semantic segmentation. In *Proceedings of the IEEE conference on computer vision and pattern recognition*, pages 580–587, 2014.
- [5] Ross Girshick. Fast r-cnn. *arXiv preprint arXiv:1504.08083*, 2015.
- [6] Shaoqing Ren, Kaiming He, Ross Girshick, and Jian Sun. Faster r-cnn: Towards real-time object detection with region proposal networks. In *Advances in neural information processing systems*, pages 91–99, 2015.
- [7] Jonathan Long, Evan Shelhamer, and Trevor Darrell. Fully convolutional networks for semantic segmentation. In *Proceedings of the IEEE conference on computer vision and pattern recognition*, pages 3431–3440, 2015.
- [8] Song Han, Huizi Mao, and William J Dally. Deep compression: Compressing deep neural networks with pruning, trained quantization and huffman coding. *arXiv preprint arXiv:1510.00149*, 2015.
- [9] Shuchang Zhou, Yuxin Wu, Zekun Ni, Xinyu Zhou, He Wen, and Yuheng Zou. Dorefa-net: Training low bitwidth convolutional neural networks with low bitwidth gradients. *arXiv preprint arXiv:1606.06160*, 2016.
- [10] Jungwook Choi, Zhuo Wang, Swagath Venkataramani, Pierce I-Jen Chuang, Vijayalakshmi Srinivasan, and Kailash Gopalakrishnan. Pact: Parameterized clipping activation for quantized neural networks. *arXiv preprint arXiv:1805.06085*, 2018.
- [11] Geoffrey Hinton, Oriol Vinyals, and Jeff Dean. Distilling the knowledge in a neural network. *arXiv preprint arXiv:1503.02531*, 2015.
- [12] Bharat Bhuvan Sau and Vineeth N Balasubramanian. Deep model compression: Distilling knowledge from noisy teachers. *arXiv preprint arXiv:1610.09650*, 2016.
- [13] Asit Mishra and Debbie Marr. Apprentice: Using knowledge distillation techniques to improve low-precision network accuracy. *arXiv preprint arXiv:1711.05852*, 2017.
- [14] Antonio Polino, Razvan Pascanu, and Dan Alistarh. Model compression via distillation and quantization. *arXiv preprint arXiv:1802.05668*, 2018.
- [15] Matthieu Courbariaux, Yoshua Bengio, and Jean-Pierre David. Binaryconnect: Training deep neural networks with binary weights during propagations. In *Advances in neural information processing systems*, pages 3123–3131, 2015.
- [16] Mohammad Rastegari, Vicente Ordonez, Joseph Redmon, and Ali Farhadi. Xnor-net: Imagenet classification using binary convolutional neural networks. In *European Conference on Computer Vision*, pages 525–542. Springer, 2016.
- [17] Fengfu Li, Bo Zhang, and Bin Liu. Ternary weight networks. *arXiv preprint arXiv:1605.04711*, 2016.

- [18] Chenzhuo Zhu, Song Han, Huizi Mao, and William J Dally. Trained ternary quantization. *arXiv preprint arXiv:1612.01064*, 2016.
- [19] Itay Hubara, Matthieu Courbariaux, Daniel Soudry, Ran El-Yaniv, and Yoshua Bengio. Binarized neural networks. In *Advances in neural information processing systems*, pages 4107–4115, 2016.
- [20] Zhaowei Cai, Xiaodong He, Jian Sun, and Nuno Vasconcelos. Deep learning with low precision by half-wave gaussian quantization. *arXiv preprint arXiv:1702.00953*, 2017.
- [21] Alex Krizhevsky, Vinod Nair, and Geoffrey Hinton. The cifar-10 dataset. *online: <http://www.cs.toronto.edu/kriz/cifar.html>*, 2014.
- [22] Olga Russakovsky, Jia Deng, Hao Su, Jonathan Krause, Sanjeev Satheesh, Sean Ma, Zhiheng Huang, Andrej Karpathy, Aditya Khosla, Michael Bernstein, et al. Imagenet large scale visual recognition challenge. *International Journal of Computer Vision*, 115(3):211–252, 2015.
- [23] Chen-Yu Lee, Saining Xie, Patrick Gallagher, Zhengyou Zhang, and Zhuowen Tu. Deeply-supervised nets. In *Artificial Intelligence and Statistics*, pages 562–570, 2015.
- [24] Itay Hubara, Matthieu Courbariaux, Daniel Soudry, Ran El-Yaniv, and Yoshua Bengio. Quantized neural networks: Training neural networks with low precision weights and activations. *arXiv preprint arXiv:1609.07061*, 2016.
- [25] Shuang Wu, Guoqi Li, Feng Chen, and Luping Shi. Training and inference with integers in deep neural networks. *arXiv preprint arXiv:1802.04680*, 2018.
- [26] Kaiming He, Xiangyu Zhang, Shaoqing Ren, and Jian Sun. Identity mappings in deep residual networks. In *European Conference on Computer Vision*, pages 630–645. Springer, 2016.
- [27] Shu-Chang Zhou, Yu-Zhi Wang, He Wen, Qin-Yao He, and Yu-Heng Zou. Balanced quantization: An effective and efficient approach to quantized neural networks. *Journal of Computer Science and Technology*, 32(4):667–682, 2017.